Mass Transfer and Pneumatic Transport Assessment in a Laboratory-Scale Photobioreactor Design for Microalgae Culture

Danna C. Forero, Liliana Ardila*

Environmental Engineering Department – ECCI University Carrera 19 # 49-20 - Bogotá - Colombia
lardilaf@ecci.edu.co

In this research, the criteria and heuristics used to design and construct a photobioreactor to cultivate microalgae on a laboratory scale are presented. Within the evaluation of the performance of the equipment, the estimation of the pressure drop in the pneumatic transport of carbon dioxide from atmospheric air was carried out, as well as the determination of the mass transfer coefficient of carbon dioxide gas in the culture broth to ensure the development of the Chlorella species in 1 L containers with bubblers of 4 different configurations. The kinetics and performance of the microalgae in the elaborated culture system were also determined. As a result, the pressure drop obtained within the Pneumatic System was 9 PSI, reflecting a relatively significant loss of feed air. The value of the highest mass transfer coefficient kLa was 0,0056 s^{-1}, indicating that it is necessary to formulate alternatives to improve the mixing of the culture broth to improve the distribution of nutrients and carbon dioxide. Finally, the biomass yield presented a value comparable with other cultivation systems proposed by different researchers.

1. Introduction

The microalgae culture is an activity of growing interest due to the diversity of benefits that these organisms can provide in fields such as nutrition, water treatment, or the generation of biofuels, high value-added products, and others (Camacho, Macedo, & Malcata, 2019) (Schaum, Mandis, Jerono, Tronci, & Meurer, 2019). Continental and marine water sources are fountains of different species of algae. However, they have a limited development due to natural growing conditions, including other competing species for nutrients and predators such as zooplankton, higher vertebrates, and other living organisms (Roldán & Ramírez, 2008). Therefore, to increase the algae biomass, a type of bioreactors called "photobioreactors" are required to provide the basic requirements at the most favorable conditions to meet the best microalgae growth.

Several photobioreactors have been designed, ranging from the open pounds like raceways which are the most commonly employed, to more complex photobioreactors design. Open pounds have large sizes to obtain a great microalgae quantity, but their build is cheap. Although, this type of photobioreactor has some disadvantages like excessive evaporation, temperature fluctuations, and a high risk of contamination (Chisti, 2012). Closed batch or continuous photobioreactors like stirred tanks, bubble column, airlift has been proposed (Kadic & Heindel, 2014) where growth and process parameters are controlled but their size is smaller than open systems, and their operation and automation costs can be pretty high (Williams, 2002)

Even though photobioreactor diversity, photobioreactors like chemical reactors are designed taking into account a set of design guidelines and heuristics that help obtain high biomass yields and thus economic benefits. Critical aspects of designing a bioreactor, including photobioreactors, are configuration, size, operation mode, and process conditions (Doran, 2013) where photobioreactor designers must select the appropriate nutrient culture medium (Watanabe, 2005), irradiance, temperature, and pH values as well as their control mechanism.

However, this is not enough since it is necessary to maintain nutrients in permanent suspension so that the microalgae can take advantage of them. Additionally, if the nutrient medium does not have a carbon source, it must be supplied in gaseous form through atmospheric air of gas cylinders.

Therefore, transport phenomena play an essential role and are associated with aeration and gas distribution processes in photobioreactors with relevant results such as the homogenization of variables in the culture medium and the increase in microalgae productivity (Doran, 2013). This work aims to analyze the air transport through a pipe net and the gas distribution in laboratory-scale photobioreactors applying the fluid mechanic and mass transfer concepts.

2. Material and Methods

2.1 Designed Photobioreactor system configuration and accessories

Photobioreactor main structure: A laboratory-scale batch photobioreactors series were installed on a three-partition shelf. Each partition holds four vessels that serve as photobioreactors.

Atmospheric air distribution system: The selected carbon source is Carbon dioxide CO_2 and is driven by an oil-free compressor with a buffer tank and water trap to ensure continuous operation during the cultivation time. The working pressure was 144.75 KPa abs (14.65 KPa man), the airflow of 6CFM, and 0.75 kW. A rubber hose of 6 mm of inner diameter carries the air between the compressor´s outlet and the inlet of a polypropylene pipe net with an inner diameter of 20 mm, installed on the shelf. This pipe transports the air to 12 ports where photobioreactor vessels were connected. All ports have an airflow regulator and a 0.22 µm PTFE membrane filter to minimize the possibility of contamination with other microorganisms and pollutants.

Light system: Each shelf partition holds two LED lamps with a manual timer which allows programming a different light-darkness period from the other partition.

Photobioreactor Vessels: Schott Duran 0.1 m^3 glass vessels were employed. The lid of the vessels has an air inlet port and two outlet ports for air and sample collection. Inlet ports are connected to glass bubblers of 4.88 x 10^{-3} m diameter with specific configuration ends (rounded hose with holes made by a thin needle, Tee configuration, and simple hole) or polymer bubbler of 0,015 m diameter and cross end to choose the one that produces the highest mass transfer coefficient. The following illustration shows the photobioreactor system configuration
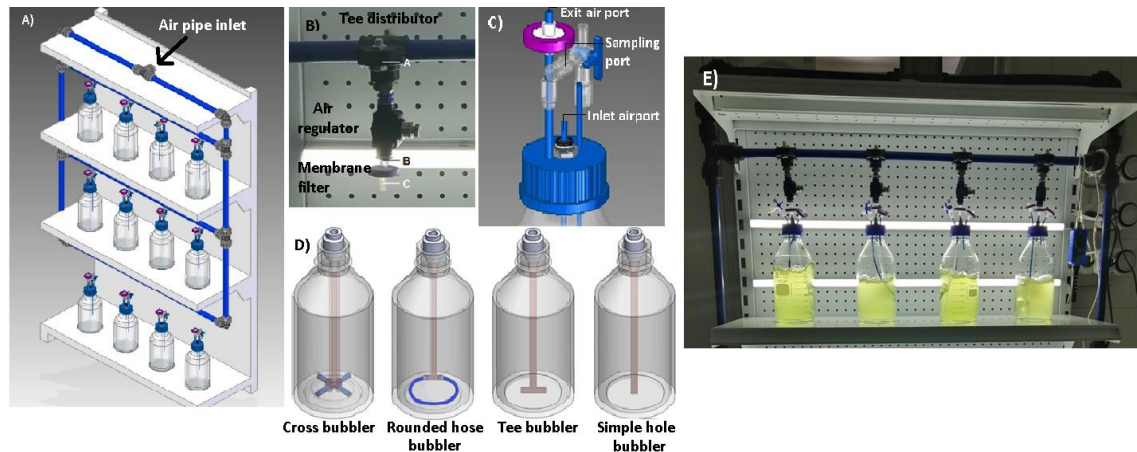

Figure 1: A) Represents the global structure of the photobioreactor system. B) Airflow pipe with flow regulator and membrane filter. C) Vessel´s lid with ports. D) Four inlet distributors of air. E) Microalgae growth..

2.2 Basic fluid properties.

Air properties: Atmospheric air density and dynamic viscosity were taken at different values from table (Mott, 2006). Gas Specific weight γ_g (N m^{-3}) was estimated by the formula

$$\gamma_g = \frac{P}{RT}$$ (1)

Where P is Absolute pressure of gas (KPa), T is the absolute temperate of gas (K), and R is the gas Constant (KPa*m^3 kmol^{-1}°K^{-1})

Bold Bassal Media Properties: A pycnometer and a capillary viscosimeter 51320 APP Nr 1040680 served to calculate density and kinetic viscosity. The surface tension was calculated with a 500 mL of BBM culture medium using Wilhelmy Method. Other properties such as specific weight and dynamic viscosity were estimated theoretically (Mott, 2006).

2.3 Pneumatic dynamic assessment.

The total head loss hL was calculated by the following formula considering two principal parts of the aeration system: 1) The compressor´s outlet to the inlet of the air pipe 2) From the air pipe inlet to the air regulator inlet. Principal head loss due to friction is associated with the first term after equal sign in (**2**, called Darcy´s model. Second and third terms after equal sign are associated with minor loss attributed to air pipe net accessories.

$$h_L = f\left(\frac{L}{D}\right)\left(\frac{v^2}{2g}\right)_p + f\left(\frac{L_e}{D}\right)\left(\frac{v^2}{2g}\right)_v + K\left(\frac{v^2}{2g}\right)_m \tag{2}$$

In this equation, v is air velocity calculated with the relation between the inner pipe area and the airflow measured with a flowmeter at different points as is shown in image B in Figure 1. F is the friction factor obtained by the Moody diagram with the estimation of the pipe Reynold´s number and its relative roughness taken from the literature (Mott, 2006). The ratio L/D relates the pipe length and its inner diameter, and K is the resistance coefficient for joints, valves, and tees, and pipe diameter changes. Pressure drop (ΔP) was calculated at different sections with equation (3), while pressure drop between airflow regulator and membrane filter was obtained experimentally with the help of a differential manometer.

$$\Delta P = \gamma_g * h_L \tag{3}$$

2.4 Mass transfer and bubble´s hydrodynamic assessment

Since the laboratory had a calibrated probe (Sparklink Pasco) to measure dissolved oxygen in aqueous media, the mass transfer coefficient for oxygen was calculated for the photobioreactor with the different bubblers, as seen in the image D in Figure 1. The Dynamic method (Doran, 2013) (Cicci, Stoller, Moroni, & Bravi, 2015) was employed quantifying the dissolved oxygen concentration ($C_{AL\,1}$) (mg/L) as the lowest oxygen concentration at the end of deaeration ($C_{AL\,2}$) (mg/L) as oxygen concentration during aeration and (C_{AL}) (mh/L) as oxygen concentration at stationary state.The following formula helped calculate the mass transfer coefficient of CO_2 in the BBM culture broth. (Fernandes, et al., 2014).

$$k_L a(CO2) = \sqrt{\frac{D_{O_2}}{D_{CO_2}}}\, k_L a(O_2) \tag{4}$$

K_{La} (CO_2) and K_{La} (O_2) are the volumetric mass transfer coefficients of CO_2 and O_2 in s^{-1}. D_{O2} and D_{CO2} are diffusion coefficients of CO_2 and O_2 at 20 °C and 25°C (cm^2 s^{-1}), obtained from (The Engineering Toolbox, 2009). Other parameters such as gas flow rate, bubble diameter, ascent rate, gas retention, and the specific interfacial area were also calculated according to (Treybal, 1980)

2.5 Cell density determination by spectrophotometer

Chlorella sp. was cultured at first in agar medium for almost a month and a half at 20°C to 25°C with a light – darkness period of 12:12. Then, microalgae was cultured in Bold Bassal liquid media **BBM** (Watanabe, 2005). Kinetic cell growth was determined by manually counting with the Neubauer Chamber and Spectrophotometry technique at a wavelength of 680 nm (Ribeiro, Arenzon, Raya, & Ferreira, 2011).

3. Results and Discussion

3.1 Pneumatic dynamic assessment.

Pneumatic parameters are shown in Table 1 to Table 2, where energy loss is calculated as the friction factor and accessory's function. Results from Table 1 show a vast difference between the head loss due to friction in the hose and the air pipe. The main factor that explains this difference is air velocity which is twelve times greater in the hose, while the friction factor is 0.56 times the friction factor of the air pipe.
Volume airflow decreased by 1.7%, while the Reynolds number decreased by 7.6% with the temperature increase due to the air density reduction in both pneumatic parts. However, the friction factor increased by 1.1% to1.5% because viscosity also increased at higher temperatures generating more flow resistance despite the above. The principal head loss diminished by 1.9% to 2.53% at higher temperatures, showing that volume airflow produced a stronger effect than the friction effect in the Darcy equation. For the minor head loss, four 90° joints, five standard tee distributors, and twelve gate valves gave a total equivalent length of 157 m. With this length, the minor loss was calculated. Table 2 shows the total loss and pressure drop at different parts of the air system.

Table 1: Major head loss calculations in the air distribution system.

Pneumatic part	Temperature (°C)	Density (Kg m^{-3})	Viscosity (Pa s)	Volume airflow (L min^{-1})	Air velocity (m s^{-1})	Reynolds number	Friction factor	Head loss (m)
1)From compressor outlet (6 mm inner diameter hose)	15	1,23	1.79 E-05	74.68	44.01	2,56 E+04	1.87E-2	615.70
	20	1,20	1.81 E-05	74.03	43.64	2.48 E+04	1.88E-2	609.60
	25	1,18	1.83 E-07	73.41	43.27	2.38 E+04	1.89E-2	600.46
2) From air pipe (20 mm inner diameter)	15	1,23	1.79 E-05	74.68	3,92	7.65 E+03	3.33E-2	5.60
	20	1,20	1.81 E-05	74.03	3.88	7.37 E+03	3.34E-2	5.53
	25	1,18	1.83 E-07	73.41	3.85	7.11 E+03	3.38E-2	5.50

Table 2: Total energy loss and pressure drop in the air distribution system.

Temperature (°C)	Major head loss (m)	Minor loss (m)	Total energy loss (m)	Specific weight N m^{-3}	Pressure drop* Kpa	Pressure drop** Kpa
15	621.30	13.44	2.08E+3	17.12	10.81	56.95
20	615.13	13.25	2.06E+3	16.81	10.52	57.24
25	605.96	13..8	2.03E+3	16.49	10.24	57.52

* Is the pressure drop from the compressor outlet to the airflow regulator inlet.
** Is the pressure drop between the airflow regulator and membrane filter.

The more significant pressure drop is associated with volume airflow loss. The flowmeter detected flow changes in A, B, and C sections as is shown in image B in Figure 1. From the compressor´s outlet, volume airflow was 74,026 L min^{-1}; thus, it was hoped that photobioreactor vessels could receive a volume airflow of 6,168 L min^{-1}. However, after Tee air splitter (A), volume airflow was 4.85 L min^{-1} the membrane filter (C), the volume airflow was 2,67 L min^{-1}, showing a volume flow reduction by 57% and a pressure loss by 88%.

3.2 Mass transfer assessment

A performance test to select the proper bubbles indicated that rounded hose and cross bubblers must be discarded. In the first one, bubbles only came out from the nearest holes from the glass straw. Thus, it does not prevent microalgae sedimentation. The second one needed an airflow above 4,06 L min^{-1} so that the air outlet would be through the four holes. However, such airflow is excessive and causes culture broth loss due to spillage. Otherwise, air came out from one or two adjoining holes, which did not allow a good bubble distribution. Additionally, both bubblers were difficult to clean and sterilize. Therefore, broth contamination risk is high.
Tee and simple hole bubblers were selected for the Oxygen mass transfer coefficient (KLa) determination. These bubblers were easy to clean, and their configuration was the most straightforward and most economical, even though they were not the most efficient. In the Tee bubbler, the gas distribution was presented frequently through one of the holes, while the simple hole configuration facilitated the air distribution in the central part of the photobioreactor but not towards the side.
The reason why the rounded hose, cross, and tee bubblers fed air sideways is the shelf-slope to prevent the flooding with the air-water that could be eliminated at a joint in the pipe. In addition, the air supply straws were not glued or rigidly adjusted since in the stage of photobioreactor cleaning; the pieces must be separated and treated with extreme care. Thus, airflow caused the misalignment of the air straws. The following figures present the Oxygen KLa estimation. This coefficient was converted to the CO_2 transfer coefficient with Equation 4.
From **Figure 2** at 20°C, each curve slope representing the oxygen transfer coefficient was determined. At lower airflow, slope ranged from 0,0056 s^{-1} to 0,0058 s^{-1} for Tee and Simple hole bubblers, respectively. At higher airflow, the slope for the T bubbler was the same, while for the simple hole bubbler, the slope dropped to 0,0028 s^{-1}. The above means that at lower airflow, air velocity is less, and bubbles gained more residence time inside photoreactors which ease the gas transfer.
At higher airflow, the performance of the simple hole bubbler decreased despite the increase in the driving force of CO_2 in the culture broth due to the gas hold-up and the predominant turbulent regime inside photobioreactors. The reason is that bubbles are bigger and gain ascends velocity near the bubbler, as seen in Table 3, which reduces the residence time of bubbles, and the mass transfer in photobioreactors (Treybal, 1980). The performance of the Tee bubbler at higher airflow was the same even though the residence time of bubbles is shorter. That is because the air came out through both holes covering a larger volume of a liquid medium with the gas, improving bubbles distribution in photobioreactors.
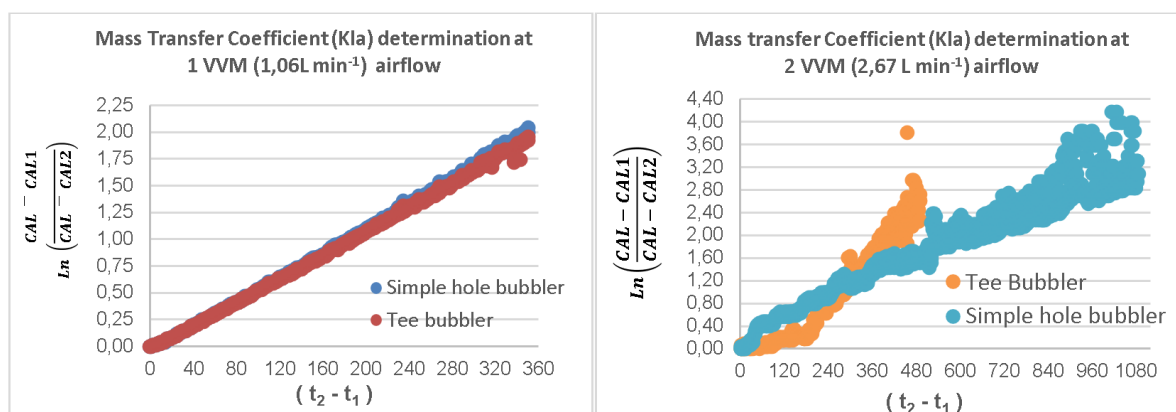
Figure 2: Oxygen transfer coefficient determination at 20°C for selected bubblers and two different airflows in VVM.

Table 3: Temperature effect on KLa (s^{-1}) value of CO_2 in selected bubblers and bubbles hydrodynamic.

| Bubbler type	Airflow	Air velocity m s^{-1}	Solubility (15°C): 0,59 ppm	Solubility (20 °C): 0,516 ppm	Solubility (25°C): 0,436 ppm
			KLa CO2 (15°C)	KLa CO2 (20°C)	KLa CO2 (25°C)
Simple hole	2 vvm	0.692	0.00301	0.00307	0.00315
Simple hole	1 vvm	0.276	0.00622	0.00636	0.00653
Tee	2 vvm	0.692	0.00601	0.00614	0.00630
Tee	1 vvm	0.276	0.00601	0.00614	0.00630
Volume airflow (L min^{-1})	Average bubble diameter (m)	Ascent velocity (m s^{-1})	Superficial gas velocity (m s^{-1})	Gas holdup	Specific interfacial area (m)
1.06	0.013	0.271	0.150	0.230	108.775
2.67	0.018	0.305	0.379	0.360	125.086
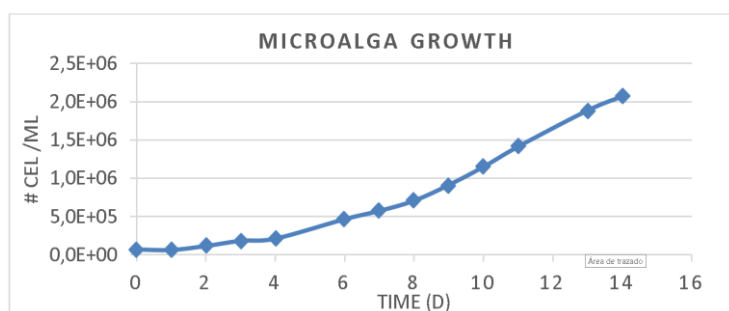
Figure 3: Chlorella sp. growth

After converting the oxygen transfer coefficient to the CO_2 transfer coefficient at different a slight increase occurred in the CO_2 transfer coefficient with the temperature increase. Thus, the temperature is directly proportional to the mass transfer coefficient at tested conditions. This happens due to the increase in internal energy that increases the kinetic energy and the mobility of the gas in the culture medium, but with the temperature increase, CO2 solubility is less. That indicates that there is an optimal temperature not only for metabolic function in microalgae biomass but for mass transfer between the gas-liquid phase. Additionally, the airflow through the bubblers gave bubbles with big diameters that increased ascend velocity and gas hold-up. That is a problem because CO_2 has little time to dissolve in the culture broth, and the gas could drag the liquid medium (Treybal, 1980) and part of oxygen could also dissolve in the culture media reducing the liquid media and microalgae growth (Doran, 2013).

Airlift photobioreactors are 50% or more efficient than the tested laboratory-scale photobioreactor, while the tested photobioreactor maintained a similar behavior with the serpentine photobioreactor (Ndiaye, Gadoin, & Gentric, 2018) in relation to the gas transfer. Despite all photobioreactor deficiencies, *Chlorella sp.* reached the stationary stage on day 14 as shown in Figure 3 and its specific growth is 0,1253 d^{-1}.

4. Conclusions

The greatest energy loss was obtained from the compressor outlet to the interconnected air pipe inlet. This head loss could be diminished by coupling a hose with a bigger diameter in order to reduce the speed of air. The selected joints of accessories are responsible for the loss of 57% of airflow and a pressure loss of almost 90% which makes the aeration system inefficient and always requires the use of a compressor with a minimum power of 1 Hp. The bubbler with the best performance was the Tee bubbler under the tested airflow because bubbles reached a larger residence time at low airflow and better dispersion inside the photobioreactor at higher airflow.

Acknowledgments

References

Camacho, F., Macedo, A., & Malcata, F. (2019, April 24). Potential industrial applications and commercialization of microalgae in the functional food and feed industries: A short review. *Marine Drugs, 17*(312), 25. doi:10.3390/md17060312

Chisti, Y. (2012). Raceways-based production of algal crude oil. In C. Posten, & C. Walter, *Microalgal biorechnology potential and production* (pp. 113 - 146). Berlin: De Gruyter.

Cicci, A., Stoller, M., Moroni, M., & Bravi, M. (2015). Mass Transfer, Light Pulsing and Hydrodynamic Stress Effects in Photobioreactor Development. *Chemical Engineering Transactions*, 235 - 240. doi:10.3303/CET1543040

Doran, P. (2013). *Bioprocess Engineering Principles* (Second ed.). Oxford: Academic Press - Elsevier.

Fernandes, B., Mota, A., Ferreira, A., Dragone, G., Teixeira, J., & Vicente, A. (2014). Characterization of split cylinder airlift photobioreactors for efficient microalgae cultivation. *Chemical Engineering Science*, 445 - 454. doi:https://doi.org/10.1016/j.ces.2014.06.043

Kadic, E., & Heindel, T. (2014). *An introduction to bioreactor hydrodynamics and gas-liquid mass transfer.* New Jersey: Wiley.

Mott, R. (2006). *Mecánica de fluidos aplicada.* Ciudad de México: Pearson.

Ndiaye, M., Gadoin, C., & Gentric, C. (2018). CO2 gas-liquid mass transfer and kLa estimation: numerical investigation in the context of airlift photobioreactor scale-up. *Chemical Engineering research and design*, 1 -19.

Ratnakar, R., Venkatraman, A., Kalra, A., & Dindoruk, B. (2020). On the prediction of gas solubility in brine solutions for applications of CO2 capture and sequestration. *Journal of Natural Gas Science and Engineering*, 1-11. doi:https://doi.org/10.1016/j.jngse.2020.103450

Ribeiro, L., Arenzon, A., Raya, M., & Ferreira, N. (2011). Algal density assessed by spectrophotometry: A calibration curve for the unicellular algae Pseudokirchneriella subcapitata. *Journal of Environmental Chemistry and Ecotoxicology, 3*, 225-228. Retrieved from www.academicjournals.org/jece

Roldán, G., & Ramírez, J. (2008). *Fundamentos de limnología neotropical.* Medellín: Universidad de Antioquia.

chaum, A., Mandis, M., Jerono, P., Tronci, S., & Meurer, T. (2019). State Estimation of Microalgae Photobioreactors: Applications to Haematococcus Pluvialis. (S. Pierucci, J. Klemes, & L. Piazza, Eds.) *Chemical Engineering Transactions*, 1423 - 1428. doi:https://doi.org/10.3303/CET1974238

The Engineering Toolbox. (2009). *Gases and compressed air*. Retrieved 01 15, 2021, from https://www.engineeringtoolbox.com/air-properties-d_156.html

Treybal, R. (1980). *Mass - Transfer operations* (Third ed.). McGraw - Hill.

Watanabe, M. (2005). Freshwater Culture Media. In R. Andersen, *Algal Culturing Techniques* (pp. 13 - 20). Elsevier - Phycological Society of America.

Williams, J. (2002). Keys to bioreactor selection. *CEP Magazine*, 34 - 41.